The Spatial-Temporal Distribution of Myeloid-Derived Immune Cells in the Wound Healing Stage of Regenerating Tail in *Scincella tsinlingensis*

Distribución Espacio-Temporal de Células Inmunitarias de Origen Mieloide en la Etapa de Cicatrización de la Cola en Regeneración de Scincella tsinlingensis

Yuwei Gao; Xinyue Wang; Xianghui Li; Tingting Shi; Zhaoting Kou & Chun Yang

GAO, Y.; WANG, X.; LI, X.; SHI, T.; KOU, Z. & YANG, C. The spatial-temporal distribution of myeloid-derived immune cells in the wound healing stage of regenerating tail in *Scincella tsinlingensis*. *Int. J. Morphol.*, 43(5):1624-1634, 2025.

SUMMARY: Inflammatory response plays an important role in tissue repair and regeneration. The tail of *Scincella tsinlingensis* was amputated with a razor blade to set up tail regeneration model. Specific cell markers of myeloid-derived monocytes, mast cell, T cell and B cell determined by single-cell transcriptome analysis of *Anolis carolinensis* were used to detect the spatial and temporal distribution of CD34+ monocytes, CMA1+ mast cells, CCR7+ T lymphocytes and CD22+ B lymphocytes in the immunoinflammatory stage of tail regeneration in *S. tsinlingensis* to bring further support to the idea of immune regulation of tail regeneration in reptiles. The results revealed distinct spatial localization patterns among different immune cell populations. Notably, CCR7+ T cells were absent from both the wound site and the dermis of proximal scales adjacent to the amputation surface, whereas CMA1+ mast cells were ubiquitously distributed across these regions. CD34+ monocytes and CD22+ B cells exhibited selective localization, being exclusively observed in the dermal layer of proximal scales near the amputation interface. Temporal analysis (0.5-7 days post-amputation, dpa) demonstrated dynamic recruitment patterns. All four immune cell types infiltrated both the wound bed and proximal dermal regions during early regeneration stages. Immune cell infiltration peaked at 5 dpa, followed by significant reduction by 7 dpa. These temporal dynamics suggest that myeloid-derived immune cells are initially recruited to the injury site through inflammatory signaling cascades, then diminish as inflammation resolves, potentially facilitating the transition from inflammatory response to regenerative processes in *S. tsinlingensis*.

KEY WORDS: Scincella tsinlingensis; Tail regeneration; Wound healing; Myeloid-derived immune cells.

INTRODUCTION

Interspecies variations in immune architectures fundamentally determine vertebrate regenerative outcomes, where immunosuppressive microenvironments emerge as prerequisite for successful tissue restoration (Degan et al., 2021). This inverse correlation between immune sophistication and regenerative capacity suggests an evolutionary trade-off in amniote development (Yang & Wu, 2014; Julier et al., 2017). Mammalian repair follows triphasic progression - inflammatory resolution (neutrophil/macrophage infiltration), proliferative expansion (stromal cell activation), and matrix remodeling - orchestrated through innate-adaptive immune crosstalk (Chaplin, 2010). Key mediators include myeloid-derived neutrophils, monocyte-differentiated macrophages, and antigen-specific T/B lymphocytes that coordinate pathogen surveillance while secreting cytokine networks

to modulate regenerative niches (Mescher et al., 2017; Tsai, 2020). Contrastingly, squamate reptiles exhibit quadripartite caudal regeneration: initial wound closure transitions to blastema formation (dedifferentiation), followed by lineage-specific differentiation and axial regrowth (Alibardi, 2014; Yang et al., 2022a). Their innate immunity employs granulocytes, complement cascades, and antimicrobial peptides, though phylogenetic conservation and functional specialization of these components in regeneration remain poorly characterized (Londono et al., 2020). Comparative analyses suggest that lizards achieve immune-competent regeneration through spatiotemporal segregation - containing inflammation during early phases while permitting immune cell participation in later remodeling stages, a regulatory balance lost in mammals.

School of Life Sciences, Shanxi Normal University, Taiyuan, Shanxi Province, P. R. China.

FUNDED. This study was supported by the National Natural Science Foundation of China (No.32470515), the Natural Science Foundation of Shanxi Province, China (No. 20210302123323) and the Natural Science Foundation of Shanxi Normal University, China (No.020820220007).

Received: 2025-05-01 Accepted: 2025-08-02

Londono et al. (2020) conducted comparative single-cell transcriptomic analyses of post-amputation immune landscapes in Anolis carolinensis and Mus musculus, revealing divergent immunophenotypic profiles. The regenerating tail and peripheral blood leukocytes of A. carolinensis exhibited unique lineage markers: monocytes (CD34, CTSS, LY86, CST3, FLT3, CTSK, CD170); basophils/mast cells (CMA1, CPA3, CTSZ, CTSD); T lymphocytes (CD247, CCR7, CD40LG, CD226); and B lymphocytes (CD22, CD8b, CD79a, CD83, JCHAIN, IGHM). Notably, A. carolinensis myeloid lineages demonstrated reduced cellular heterogeneity compared to murine counterparts. Functional convergence was observed in phagocytic activity: peripheral monocytes and heterophils/mast cells in A. carolinensis substitute neutrophil-like functions seen in mammals. Strikingly, A. carolinensis mononuclear cells expressed hematopoietic progenitor markers (CD34) while lacking macrophageassociated markers (CD68, CD11b). The substantial recruitment of monocyte-derived macrophages during regeneration suggests their critical role in reptilian tissue repair. Comparative evolutionary analysis highlights a key divergence: while mammals evolved specialized myeloid subsets, squamates retain ancestral phagocyte plasticity optimized for regenerative contexts. However, the mechanistic contribution of monocytes to Lacertilia regeneration remains unresolved, warranting further investigation into lineage-specific immune adaptations.

The regenerating lizard tail blastema exhibits dynamic immune cell polarization, with M1/M2 macrophages and Tregs expressing lineage-specific markers that differentially regulate regenerative success versus failure. Autoradiographic and immunohistochemical analyses reveal arginase-positive M2-like macrophages in Podarcis muralis blastemas, suggesting their proregenerative role through anti-inflammatory modulation (Alibardi, 2020). Concurrent detection of Dab2 and Foxp3 immunoreactivity further confirms localized immunosuppressive microenvironments mediated by Treg populations during reptilian tissue repair (Alibardi, 2022). Contrastingly, CD3+/CD5+/MHCII+ cell infiltration in amputated limbs correlates with fibrotic scarring, highlighting divergent immune responses between regenerative and non-regenerative appendages (Alibardi, 2024). While regeneration studies span over 30 ovoviviparous species across six families (e.g., A. carolinensis, Eublepharis macularius, Gekko japonicus), investigations into Scincella tsinlingensis caudal regeneration offer unique insights into post-autotomy molecular adaptations (Zhao et al., 2020; Yang et al., 2022a,b). Crucially, the wound healing phase determines regenerative competence through balanced immune

recruitment – where excessive inflammatory cell activation disrupts organ restitution, while controlled leukocyte engagement facilitates structural/functional recovery. To elucidate vertebrate regeneration immunology, spatial-temporal profiling of CD34+ monocytes, CMA1+ mast cells, CCR7+ T cells, and CD22+ B lymphocytes was performed in *S. tsinlingensis* regenerates using immunohistochemistry. These findings delineate conserved *versus* species-specific immune checkpoints, providing mechanistic evidence for the hypothesis that reptilian regeneration depends on phased immunomodulation rather than systemic immunosuppression (Alibardi, 2024).

MATERIAL AND METHOD

Experimental animal. The Lizards *S. tsinlingensis* were collected from forest region in Taiyue Mountain, Shanxi, China (36°21′-36°45′N, 110°40′-112°21′E). These lizards were housed at a soil-filled terrarium under an ambient humidity of 40 %-60 %, photoperiod of 10 h at 24 °C in the daytime and 14 h at 19 °C at night. *Tenebrio molitor* larvae and tap water were given daily to ensure their normal life activities. Experiments pertinent to animals were carried out according to animal care guidelines of the ethical committee of Shanxi Normal University.

Sampling and treatment. Based on the snout-vent length (SVL), 48 male and female adult *S. tsinlingensis* (4.8 cm \leq SVL \leq 5.7 cm) were randomly divided into 6 groups. The tail regeneration model was amputated with a razor. The lizards were placed in a 4 °C refrigerator for 20 min, cut with a sterilized single blade 2 cm away from the cloaca, and raised in different incubators. The lizards at 0 dpa, 0.5 dpa, 1 dpa, 3 dpa, 5 dpa and 7 dpa were selected to cut the tail, 0.5 cm from the tail stumps to collect the regenerated tail samples.

Paraffin section preparation. Samples were fixed in 4 % paraformaldehyde for 3 days, and rinsed with PBS (pH: 7.2-7.4) and distilled water for 3×20 min, then decalcified in JYBL-I decalcification solution for 1-3 days. The samples were dehydrated in ethanol 50 %, 70 %, 80 %, 90 % and 100 %, and then embedded in wax at 55 °C. Finally, the wax blocks were sectioned using a microtome at 10 μ m of thickness, dehydrated in ethanol 50 %, 70 %, 90 % and 100 %, and then embedded in wax at 55 °C. The sections were attached on gelatin-chromoallume coated glass slides, dried on a warm plate at 40-50 °C for 72 h, and stored at room temperature.

Immunohistochemical staining. After dewaxing and rehydration, the sections were immersed in freshly configured $3 \% H_2O_2$ for 30 min, and then the sections were

rinsed in PBS buffer for 3×5 min/ time. The compound digestive solution was added on the sections and placed at room temperature for 15 min to repair the antigen. Then, the sections were immersed in PBS buffer for 3×5 min/ time, treated with 0.2 % Triton X-100 for 10 min, and 5 % bovine serum albumin to block non-specific binding sites. The sections were incubated overnight at 4 °C with the first antibodies, rabbit anti-mouse CD34, CMA1, CCR7 and CD22 (1:100, Boster, Wuhan, China), then immersed in PBS buffer for 3×5 min/time. Biotin labeled goat antirabbit IgG (Boster, Wuhan, China) was added and incubated at 37 °C for 30 min, then incubated with streptomavidin peroxidase complex (Boster, Wuhan, China) at 37 °C for 30 min. Staining was visualized using 0.1 % diaminobenzidine (DAB) solution in 0.1 % hydrogen peroxide in PBS incubated for 5 min. The immunocytochemical stain was done using PBS instead of an antibody in blank control.

Data measurement and statistics. Immunopositive cells were counted, 3 images were randomly selected under a 40-fold mirror. Referring to the mouse HSK cell counting method, the mean number of positive cells \pm standard deviation (Mean \pm SD) indicates the number of positive cells in different days after tail amputation (Wu *et al.*, 2014). Statistical analyses were performed using SPSS 13.0 (IBM Corp.), with intergroup comparisons conducted through one-way ANOVA followed by Tukey's *post hoc* testing. Differences achieving p < 0.05 were considered statistically significant.

RESULTS

Immunolocalization of immune cells in inflammatory phase

Monocyte (CD34). The expression of CD34+ monocyte cells was very low in the wound site and the dermis of proximal scale to the stump surface at 0 days postamputation (Fig. 1a, b). The expression of CD34+ monocyte cells was detected in the wound site and the dermis of proximal scale to the stump surface at 0.5 dpa (Fig. 1c, d). The expression of CD34+ monocyte cells was very high in the wound site and the dermis of proximal scale to the stump surface in the healing time (Fig. 1). The expression of CD34+ monocyte cells was detected in the original tail muscle tissue near the wound at 5 dpa and 7 dpa. Compared with other time points, the expression of CD34+ monocytes was decreased in the wound site and the dermis of proximal scale to the stump surface at 7 dpa (Fig. 1k, 1). These results indicated that a large number of monocytes was recruited to the wound site after tail amputation, which phagocyted invasive organisms, cell

debris and other apoptotic cells to prevent infection of the wound site after tail amputation. Monocytes showed obvious phenotypic and functional changes under the effect of tissue microenvironment, and differentiated into macrophages. At the same time, monocytes and macrophages could actively regulate the process of tissue healing. The decrease of monocytes at the wound site at 7 dpa was consistent with the transcriptome results.

CMA1+ mast cells. CMAL-labeled mast cells were positively expressed at every time point of the inflammatory phase. The expression of CMA1+ mast cells was detected in connective tissue, muscle tissue and dermis under the wound site and proximal scale to the stump surface at 0 dpa (Fig. 2a, b). The expression of CMA1+ mast cells increased in the connective tissue and dermis below the wound (Fig. 2c, d), and decreased in the muscle tissue with sporadic distribution at 0.5 dpa. The expression of CMA1+ mast cells was neatly arranged in the connective tissue near the wound site at 1 dpa (Fig. 2e, f). The expression of CMA1+ was very high in the wound site and its underlying connective tissue (Fig. 2g, i), and in the dermis of proximal scale to the stump surface (Fig. 2h, j) at 3 dpa and 5 dpa. At 7 dpa, CMA1+ cells were highly expressed in connective tissue and muscle tissue in the wound site, but were negative in dermis (Fig. 2k, 1). These results indicate that mast cells are widely distributed in connective tissue and dermis, and not only participate in congenital immunity and limb protection in tail amputation regeneration of lizards, but also may play a role in homeostasis maintenance in normal physiological activities.

CD22 + B cells. CD22+ B cells were not distributed in the wound site at 0 dpa, but were expressed in the dermis of proximal scale to the stump surface (Fig. 3a, b). The connective tissue in the wound site expressed a high level of CD22+ B cells, whereas muscle cells showed comparatively low levels at 0.5dpa (Fig. 3c). The density of CD22+ B cells at 1 dpa was lower than that of 0.5 dpa in the wound site (Fig. 3e), however, the density of CD22+ at 0 d was consistent with that at 0.5 d in the dermis of proximal scale to the stump surface (Fig. 3b, d, f). While positive cells increased in the connective tissue below the wound at 3 dpa, and were close to the wound (Fig. 3g). At 5 dpa, the positives were more concentrated in the wound site (Fig. 3i), and CD22+ B cells were also distributed in the dermis of proximal scale to the stump surface. However, positive expression decreased overall at 7 dpa (Fig. 3k), and almost no positive expression was observed in dermal cells (Fig. 31). This suggests that CD22+ B cells gradually migrate to the wound site during inflammation and promote wound healing.

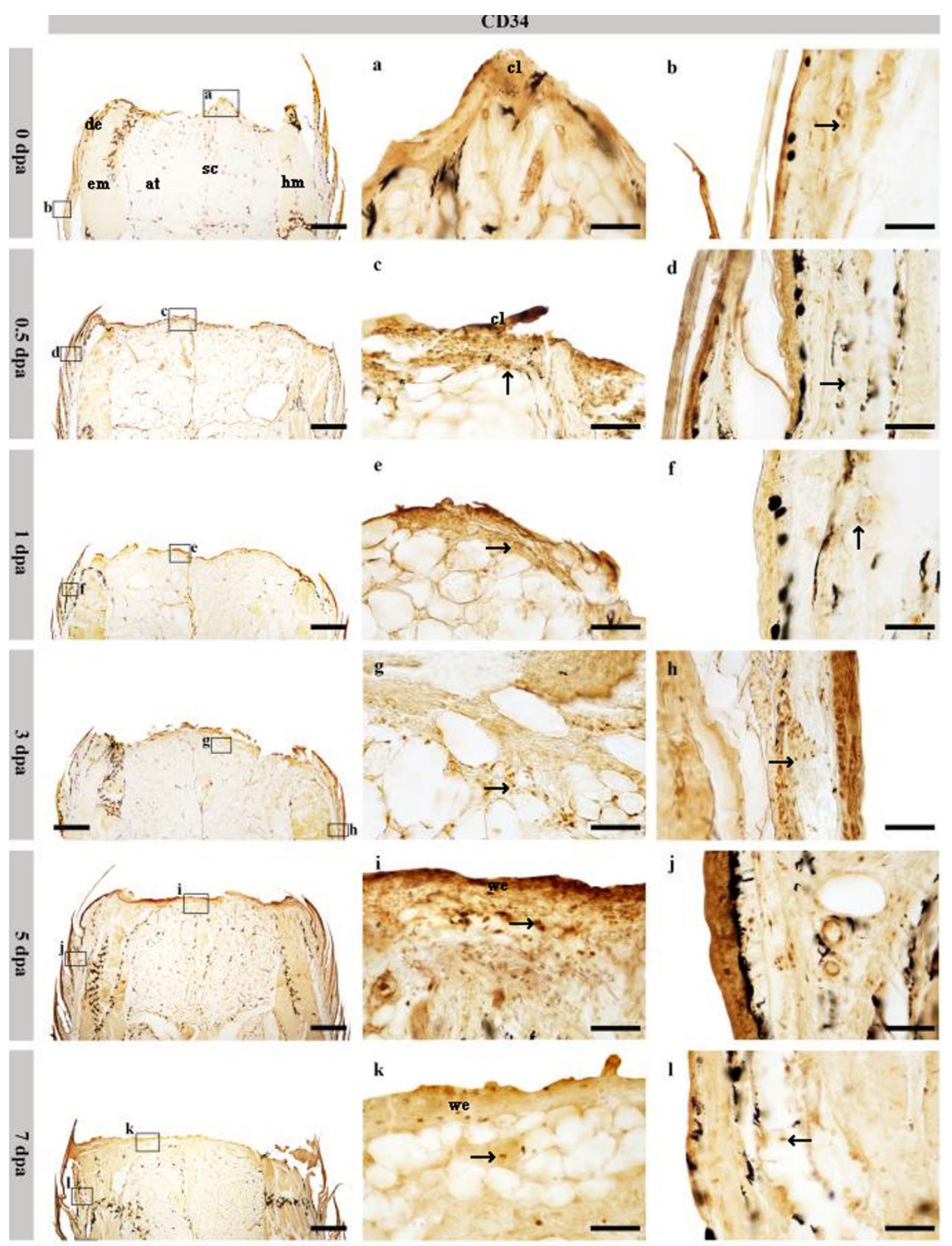


Fig. 1. Immunolocalization of CD34+ monocytes in the inflammatory stage of *S. tsinlingensis*. Immunolocalization of the monocytes in *S. tsinlingensis* at 0 - 7 dpa were characterized using CD34 antibody, bar=100 μ m. The tail at 0 dpa was treated as a control group. Figures a-b, c-d, e-f, g-h, i-j and k-l respectively indicate the localization and number of CD34+ monocytes (arrow) according to their corresponding time both at the wound site (a, c, e, g, i, k) and the squamousdermis (b,d, f, h, j, l), bar=20 μ m. The expression of positive cells at 0 dpa is low, but increased at 0.5-7 dpa. Compared with the proliferating phase of positive cells, the CD34+ monocytes is relatively reduced, at: adipose tissue; cl: clot; de: dermis; em: epaxial musculature; hm:hypaxial musculature; sc: spinal cord; we: wound epithelium.

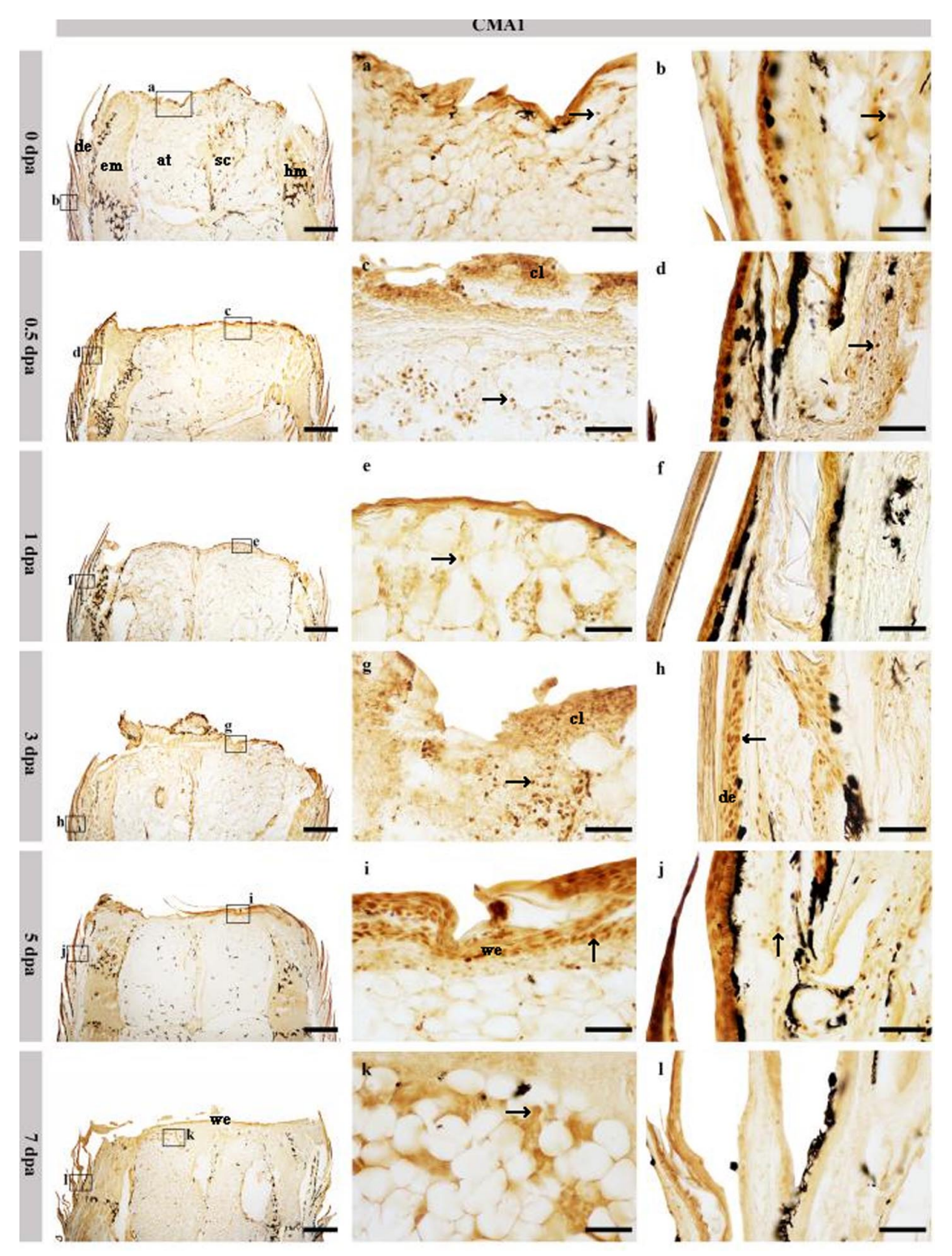


Fig. 2. Immunolocalization of CMA1+ mast cells in the inflammatory stage of *S. tsinlingensis*. Immunolocalization of the mast cells in *S. tsinlingensis* at 0 - 7 dpa were characterized using CMA1 antibody, bar=100 μ m. 0 d was treated as a control group. Figures a-b, c-d, e-f, g-h, i-j and k-l respectively indicate the localization of CMA1+ mast cells (arrow) according to their corresponding time both at the wound site (a, c, e, g, i, k) and the squamous dermis (b, d, f, h, j, l), bar=20 μ m. at: adipose tissue; cl: clot; de: dermis; em: epaxial musculature; hm:hypaxial musculature; sc: spinal cord; we: wound epithelium.

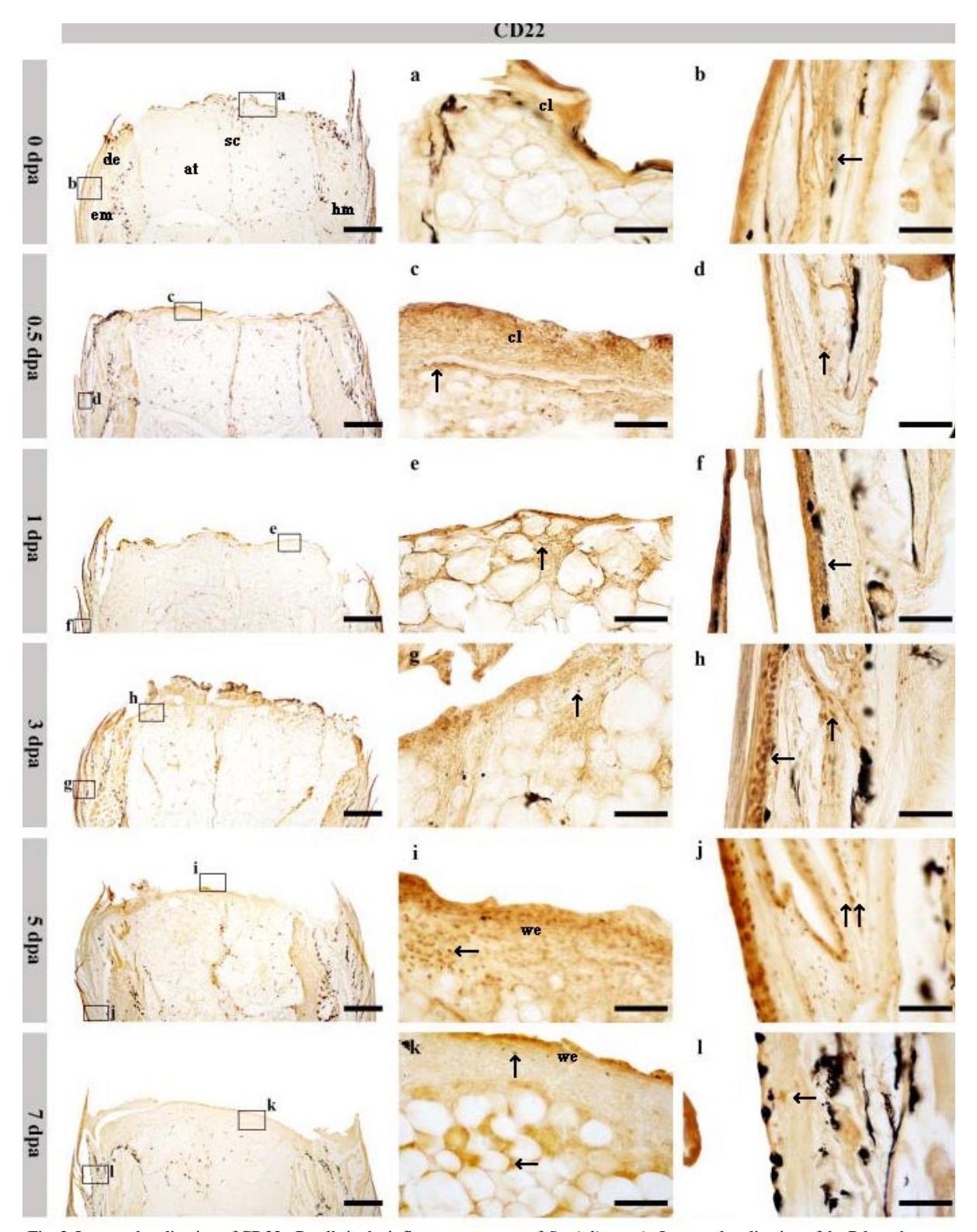


Fig. 3. Immunolocalization of CD22+B cells in the inflammatory stage of *S. tsinlingensis*. Immunolocalization of the B lymphocytes in *S. tsinlingensis* at 0 - 7 dpa were characterized using CD22 antibody, bar=100 μ m. 0 d was treated as a control group. Figures a-b, c-d, e-f, g-h, i-j and k-l respectively indicate the localization of CD22 positive cells (arrow) according to their corresponding time both at the wound site (a, c, e, g, i, k) and the squamous dermis (b, d, f, h, j, l), bar=20 μ m. at: adipose tissue; cl: clot; de: dermis; em: epaxial musculature; hm:hypaxial musculature; sc: spinal cord; we: wound epithelium.

CCR7+ T cells. The expression of CCR7+ T cells was very low in the wound site at 0.5 dpa (Fig. 4c, d). CCR7+ T cells were expressed in the wound site and its underlying connective tissue at 1 dpa and 3 dpa (Fig. 4e-h), and the expression of CCR7+ T cells was higher than that at 0.5 dpa, but that was less than the expression of CD22+ B cells, CD34+ monocytes and CMA1+ mast cells. CCR7+ T cells were mainly distributed in the connective tissue and muscle tissue under the wound site and in the dermis of proximal scale to the stump surface (Fig. 4i, j). The expression of CCR7+ T cells was low in the dermis of proximal scale to the stump surface at 7 dpa (Fig. 4k, 1). These results indicated that T lymphocytes were recruited less in the initial stage of inflammation and expressed less in the whole stage of inflammation. T cells are not activated immediately after tail amputation, but arrive in the tissue microenvironment after the action of other inflammatory cell phases, release a large number of cytokines and growth factors to promote wound healing after tail amputation regeneration, and play an important role in tissue repair and regeneration.

Quantitative statistical results of immune cells. The statistical results indicated that the expression of CD34+ monocytes in the wound site and the dermis of proximal scale to the stump surface showed the same trend of change, first increasing and then decreasing. The expression of CD34+ in the wound site had an upward trend until it reached 123.16 \pm 12.50 at 5 dpa, and then decreased to 46.59 ± 9.07 . The expression of CD34+ in the dermis of proximal scale to the stump surface reached a maximum of 91.68 \pm 6.66 at 5 dpa after tail amputation. During the inflammatory phase, more CD34+ monocytes were accumulated in the wound site than in the dermis of proximal scale to the stump surface (Fig. 5A), indicating that CD34+ monocytes rapidly accumulated in the wound site, and the inflammation began to subside at 5 dpa. The expression of CMA1+ mast cells in the wound site and the dermis of proximal scale to the stump surface showed the same trend of change, which began to increase after tail amputation and decreased obviously at 1 dpa, and increased again at 3 dpa, it increased to 68.53 ± 6.80 at 3 dpa, which was similar to that on the 0.5 day, and then showed a decreasing trend. The expression of CMA1+ mast cells in the wound site was also higher than that in the dermis of proximal scale to the stump surface (Fig. 5B). It is suggested that CMA1+ mast cells exist in the original tail tissue and the expression of CMA1+ increases after tail amputation until the inflammatory reaction decreases.

The expression of CD22+ B cells showed different trends in the wound site and the dermis of proximal scale to the stump surface. The positive cells at the wound site

increased significantly at 0.5 dpa, and then decreased, reaching the maximum of 137.57 ± 7.77 at 5 dpa. The positivecells in the wound site after tail amputation were significantly more than those in the dermis of proximal scale to the stump surface, indicating that CD22+ B cells also accumulated in the wound site after tail amputation, and then decreased with the regression of inflammation. The change trend of CCR7+T cells in the wound site and dermis of proximal scale to the stump surface was first increased and then decreased, and the maximum value was reached at 5 dpa, with 93.65 ± 10.02 in the wound site and $38.68 \pm$ 6.66 in the dermis of proximal scale to the stump surface. The expression of CCR7+ T cells was low in the early inflammation after tail amputation. At 0.5 dpa, the expression of CMA1+ mast cells in the wound was the same as that in the dermis of proximal scale to the stump surface, the expression of CMA1+ mast cells in the wound site was significantly higher than that in the dermis of proximal scale to the stump surface.

DISCUSSION

The immune regulation following appendage loss critically determines the balance between fibrotic scarring and regenerative repair (Vonk et al., 2023). Upon injury, innate immune mechanisms are rapidly activated, mobilizing neutrophils, monocytes, and other immune effectors to clear cellular debris and neutralize microbial threats. While controlled inflammation is essential for wound healing, its timely resolution represents a pivotal regulatory checkpoint. Persistent inflammatory signaling frequently drives pathological fibrosis rather than functional restoration, as evidenced in mammalian wound healing models (Landén et al., 2016). Notably, regenerative species exhibit precise immunomodulatory control post-injury, where maintained immunological equilibrium - neither excessive suppression nor prolonged activation - creates a permissive microenvironment for tissue regeneration. Squamates provide unique insights into this regulatory paradigm. Despite sharing fundamental immunological architectures with mammals, including V(D)J recombination-mediated antibody diversification, lizards demonstrate attenuated adaptive immune responses and delayed inflammatory resolution (Londono et al., 2020). This distinctive immunological profile, coupled with their capacity for extensive appendage regeneration through blastema formation, positions squamates as strategic models for investigating inflammation-regeneration interplay. The inherent moderation of their immune reactivity may establish an optimal immunological niche favoring complex tissue regeneration - an evolutionary adaptation largely absent in mammals but conserved in regenerating vertebrates (Vonk et al., 2023).

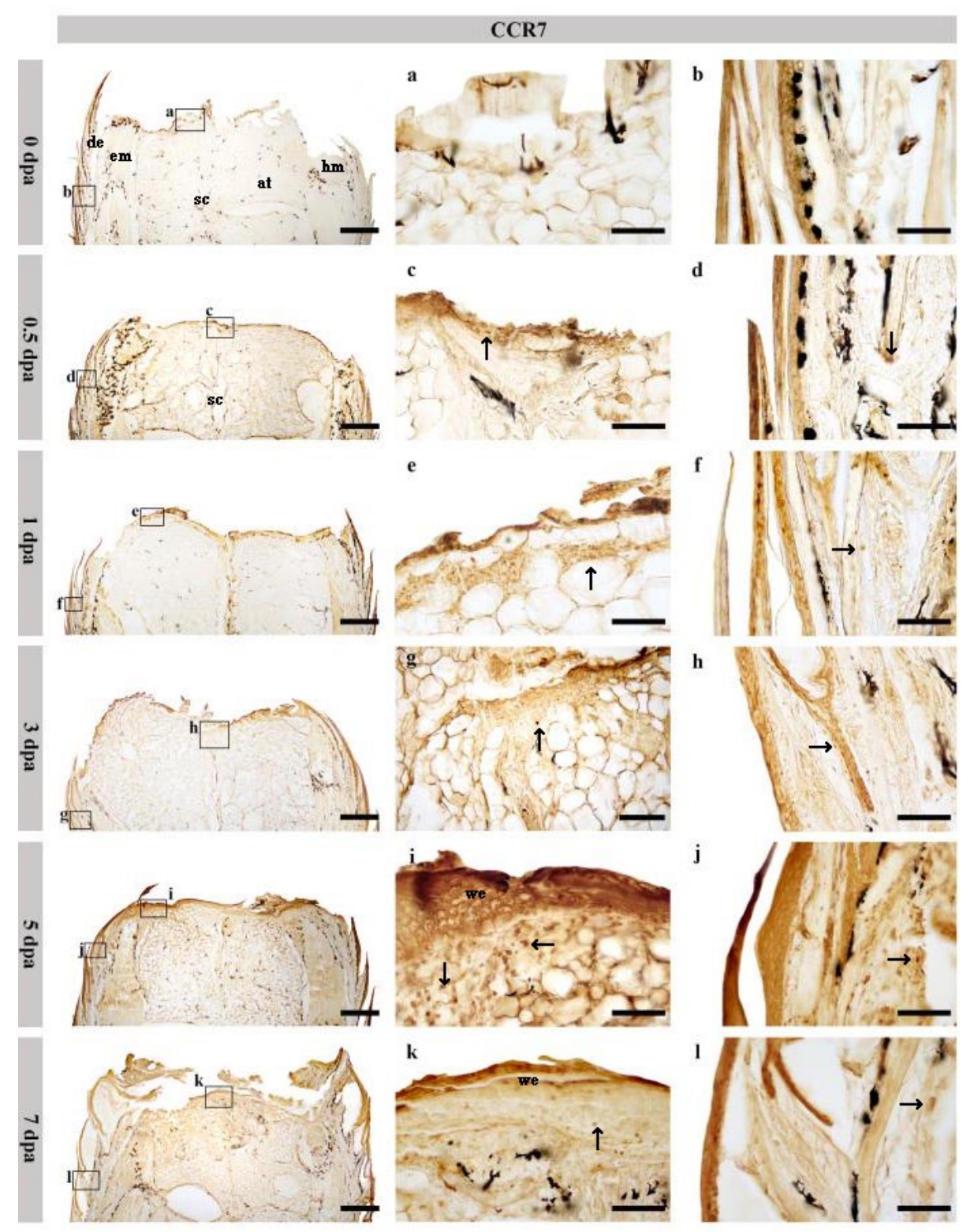


Fig. 4. Immunolocalization of CCR7+ T cells in the inflammatory stage of *S. tsinlingensis*. Immunolocalization of the T lymphocytes in *S. tsinlingensis* at 0 - 7 dpa were characterized using CCR7 antibody, bar=100 μ m. 0 d was treated as a control group. Figures a-b, c-d, e-f, g-h, i-j and k-l respectively indicate the localization of CCR7+ T cells (arrow) according to their corresponding time both at the wound site (a, c, e, g, i, k) and the squamous dermis (b, d, f, h, j, l), bar=20 μ m. at: adipose tissue; cl: clot; de: dermis; em: epaxial musculature; hm:hypaxial musculature; sc: spinal cord; we: wound epithelium.

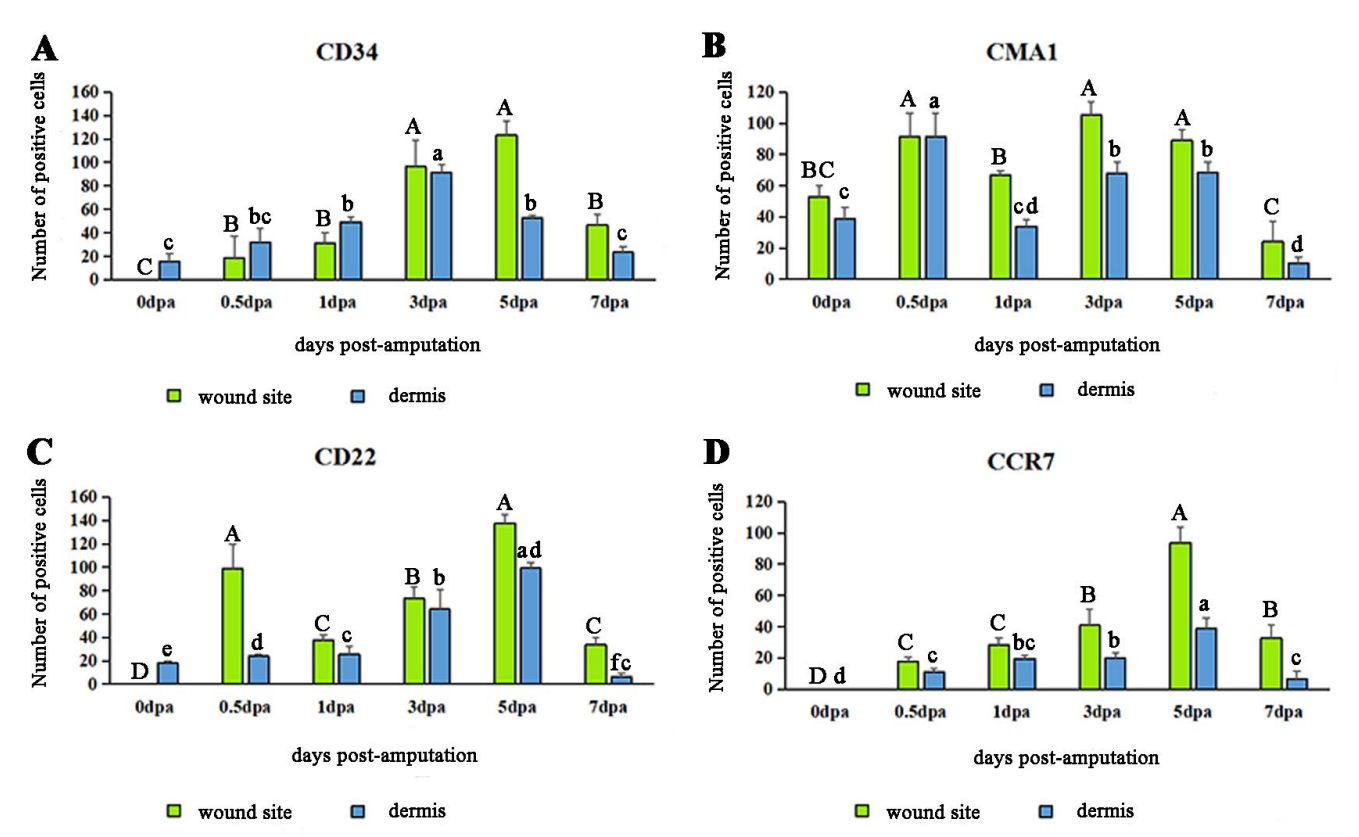


Fig. 5. Quantitative statistics of four immune cells in the inflammatory stage of *S. tsinlingensis*. Identical lowercase superscripts denote statistically comparable immunopositive cell densities at wound sites (p > 0.05), while shared uppercase letters indicate non-significant differences in dermis (p > 0.05; one-way ANOVA with Tukey's multiple comparisons).

Notably, squamate B cells exhibit dual functionality through phagocytic activity while serving innate immune roles. This robust innate immune architecture provides adequate microbial defense during early life stages, potentially explaining the evolutionary persistence of attenuated adaptive immunity in these vertebrates. Post-autotomy scarless healing initiates rapidly in lizards, serving dual functions of wound stabilization and prevention of infection/desiccation. Tail loss intrinsically activates monocyte/macrophage lineage recruitment, which orchestrates both tissue repair and subsequent regenerative processes. Vertebrate regeneration models consistently demonstrate macrophage infiltration patterns, with dense populations observed beneath wound epithelia and within injured tissues post-amputation (Daponte et al., 2021). In S. tsinlingensis, four myeloid-derived cell types - CD34+ monocytes, CMA1+ mast cells, CD22+ B cells, and CCR7+ T cells - are sequentially recruited to amputation sites during inflammatory phase progression. Comparative analyses reveal distinct healing mechanisms: While MHCII/ CD3/CD5 immunolocalization in P. muralis amputated appendages indicates fibrotic programming (Alibardi, 2024), the coordinated mobilization of specialized immune subsets in S. tsinlingensis suggests an evolutionarily optimized pathway favoring regeneration over scarring.

Monocytes, hematopoietic derivatives of bone marrow stem cells, circulate as versatile innate immune effectors. These heterophilic cells exhibit remarkable phenotypic plasticity, dynamically adapting to microenvironmental cues and pathogenic challenges (Das et al., 2015). Post-injury analysis (1-3 dpa) reveals sequential myeloid activity: initial neutrophil infiltration precedes monocyte recruitment to wound sites, where differentiation into functional macrophages occurs. Early-phase M1 macrophages dominate the pro-inflammatory stage through phagocytic clearance (via matrix metalloproteinases) and cytokine production (IL1 β , TNF- α , IL6), while coordinating secondary immune cell recruitment. Subsequent polarization into M2 macrophages orchestrates tissue remodeling via anti-inflammatory mediators (IL10, TGF-β, arginase-2) and mitogenic factor secretion (Vonk et al., 2023). Evolutionary insights from salamander limb regeneration demonstrate monocyte-derived osteoclast specialization during blastema formation, confirming monocytic subpopulation involvement in regenerative pathways (Fischman & Hay, 1962). Mast cells, originating from hematopoietic precursors through systemic migration, modulate innate responses via effector molecule release (histamine, proteases) that recruits eosinophils and monocytes (Julier et al., 2017). While mast cell accumulation correlates

with fibrotic outcomes in CNS injuries and chronic wounds through acute inflammation exacerbation (Skaper *et al.*, 2014), their paradoxical role emerges through context-dependent mediator release. Strategic modulation of mast cell activity - balancing pro-regenerative cytokine production against pro-fibrotic effector molecules - presents therapeutic potential for steering repair processes toward regeneration rather than scarring (Julier *et al.*, 2017).

T lymphocytes critically regulate tissue repair processes through spatiotemporal secretion of cytokines and growth factors that modulate healing outcomes. Regulatory T cells (Tregs) emerge as pivotal immunomodulatory mediators, producing anti-inflammatory cytokines (IL-10, TGF-β) to suppress excessive inflammation while coordinating regenerative cascades (Zaiss et al., 2013). Evolutionary conservation of this mechanism is evidenced in Danio rerio, where Treg-like cell populations are indispensable for spinal cord, cardiac, and retinal regeneration post-injury (Tsai, 2020). Tissue-resident Tregs localized in visceral adipose, skeletal muscle, and lamina propria uniquely express epidermal growth factor receptor (EGFR). This molecular signature enables cross-talk with mast cell-derived delmodulin, creating a self-reinforcing loop: EGFR signaling maintains Treg retention at injury sites, while Treg proliferation augments delmodulin production a biochemical prerequisite for successful regeneration (Julier et al., 2017). B lymphocytes, originating from bone marrow precursors, exhibit underappreciated osteoimmunological functions. IgM-positive B cell subsets contribute to skeletal repair through osteoprotectin (OPN) secretion, directly accelerating osteogenic differentiation and bone matrix deposition (Könnecke et al., 2014). This immunologically mediated osteogenesis bridges hematopoietic and musculoskeletal systems, revealing novel therapeutic targets for bone regeneration (Kular et al., 2012).

Lizard blastema cells and immature somatic tissues demonstrate remarkable inflammatory resistance postamputation. Deciphering this self-limiting inflammatory mechanism during caudal regeneration could unveil therapeutic strategies for human tissue repair (He et al., 2021). In A. carolinensis, tail regeneration progresses through distinct phases: The initial inflammatory stage (0.5-1 dpa) transitions abruptly at 2 dpa into a proliferation-dominated phase (1-5 dpa), marked by T lymphocyte-mediated immunomodulation replacing acute inflammation. This inflammatory resolution coincides with transcriptional reprogramming that synchronizes cellular proliferation, developmental pathway reactivation, and accelerated epithelial closure. Mechanistically, A. carolinensis amputation triggers rapid phagocyte mobilization, with macrophage recruitment kinetics showing accelerated

infiltration compared to murine models. Elevated expression of tissue remodeling proteases (CSTK, MMP2) at injury sites appears essential for successful reptilian regeneration (Londono *et al.*, 2020). Comparative ultrastructural analyses in *P. muralis* reveal that recurrent amputations induce blastema-level immunopathology: granulocyte/macrophage/lymphocyte infiltration correlates with fibrinoid deposition and fibrotic scarring (Alibardi, 2018). These findings suggest an evolutionary trade-off between enhanced immune competence and regenerative capacity in amniotes. The precise crosstalk among blastema progenitors, immune effectors, and mesenchymal compartments during regeneration remains undefined, necessitating further investigation into these cellular tripartite interactions (Daponte *et al.*, 2021).

The efficient innate immune response in lizards appears to constrain inflammatory propagation, particularly following autotomy-induced tissue separation without residual damage. This regulatory mechanism correlates with attenuated activation of inflammatory mediators and immune effectors during regenerative processes. While amphibians and lizards typically exhibit transient inflammation (<72 hours) during physiological regeneration, persistent immune activation occurs under pathological conditions such as thermal cauterization or repetitive amputation injuries. Following initial innate immune defense, sustained microbial challenges or chronic inflammation may trigger adaptive immunity mediated through B/T lymphocyte networks. Lymphocytic infiltration observed during caudal regeneration suggests dual functionality: antibody production and blastema surveillance through activated T-cell populations, potentially serving as fail-safe mechanisms against regenerative inhibition under persistent irritative conditions (Alibardi, 2014). Evolutionary analysis reveals a critical dichotomy: terrestrial vertebrates' regenerative failure primarily stems from hyperactivation of pro-inflammatory macrophages and neutrophils driving rapid fibrotic encapsulation, whereas effective reptilian regeneration maintains precise immune modulation (Alibardi, 2024). This immunological balance paradigm emphasizes that regeneration competence inversely correlates with inflammatory intensity, positioning immune checkpoint regulation as a pivotal determinant of regenerative success across amniotes.

ACKNOWLEDGEMENTS.

This study was supported by the National Natural Science Foundation of China (No.32470515), the Natural Science Foundation of Shanxi Province, China (No. 20210302123323) and the Natural Science Foundation of Shanxi Normal University, China (No.020820220007).

GAO, Y.; WANG, X.; LI, X.; SHI, T.; KOU, Z. & YANG, C. Distribución espacio-temporal de células inmunitarias de origen mieloide en la etapa de cicatrización de la cola en regeneración de *Scincella tsinlingensis*. *Int. J. Morphol.*, 43(5):1624-1634, 2025.

RESUMEN: La respuesta inflamatoria desempeña un papel crucial en la reparación y regeneración tisular. Para establecer un modelo de regeneración caudal en Scincella tsinlingensis, se realizó la amputación de la cola mediante hoja de afeitar. Utilizando marcadores celulares específicos (monocitos de origen mieloide, mastocitos, células T v B) identificados mediante análisis de transcriptoma unicelular en Anolis carolinensis, se investigó la distribución espacio-temporal de monocitos CD34+, mastocitos CMA1+, linfocitos T CCR7+ y linfocitos B CD22+ durante la fase inmunoinflamatoria de la regeneración caudal en S. tsinlingensis, aportando evidencia adicional sobre la regulación inmunológica de la regeneración en reptiles. Los resultados revelaron patrones de localización espacial distintivos entre las poblaciones de células inmunes. Notablemente, las células T CCR7+ estuvieron ausentes tanto en el sitio de la herida como en la dermis de las escamas proximales adyacentes a la superficie de amputación, mientras que los mastocitos CMA1+ mostraron distribución ubicua en estas regiones. Los monocitos CD34+ y las células B CD22+ exhibieron localización selectiva, limitándose exclusivamente a la capa dérmica de las escamas proximales cercanas a la interfaz de amputación. El análisis temporal (0,5-7 días post-amputación, dpa) demostró dinámicas de reclutamiento celular. Las cuatro poblaciones inmunes infiltraron tanto el lecho de la herida como las regiones dérmicas proximales durante las etapas tempranas de regeneración. La infiltración celular alcanzó su punto máximo a los 5 dpa, seguido de una disminución significativa a los 7 dpa. Estas dinámicas sugieren que las células inmunes mieloides son inicialmente reclutadas al sitio lesional mediante cascadas de señalización inflamatoria, para luego reducirse conforme la inflamación se resuelve, facilitando potencialmente la transición desde la respuesta inflamatoria hacia los procesos regenerativos en S. tsinlingensis.

PALABRAS CLAVE: Scincella tsinlingensis; Regeneración de la cola; Cicatrización de heridas; Células inmunitarias de origen mieloide.

REFERENCES

- Alibardi, L. Histochemical, biochemical and cell biological aspects of tail regeneration in lizard, an amniote model for studies on tissue regeneration. *Prog. Histochem. Cytochem.*, 48(4):143-244, 2014.
- Alibardi, L. Tail regeneration reduction in lizards after repetitive amputation or cauterization reflects an increase of immune cells in blastemas. *Zool. Res.*, *39*(*6*):413-23, 2018.
- Alibardi, L. Autoradiography and immunolabeling suggests that lizard blastema contains arginase-positive M2-like macrophages that may support tail regeneration. *Ann. Anat.*, 231:151549, 2020.
- Alibardi, L. Immunoreactivity for Dab2 and Foxp3 suggests that immunesuppressive cells are present in the regenerating tail blastema of lizard. *Acta Zool.*, 103(4):389-401, 2022.
- Alibardi L. Immunolocalization of CD3, CD5 and MHCII in amputated tail and limb of the lizard *Podarcis muralis* marks a scarring healing program. *Acta Zool.*, 105(2):189-204, 2024.
- Chaplin, D. D. Overview of the immune response. J. Allergy. Clin. Immunol., 125(2 Suppl. 2):S3-23, 2010.
- Daponte, V.; Tylzanowski, P. & Forlino, A. Appendage regeneration in vertebrates: what makes this possible? *Cells*, 10(2):242, 2021.
- Das, A.; Sinha, M.; Datta, S.; Abas, M.; Chaffee, S.; Sen, C. K. & Roy, S. Monocyte and macrophage plasticity in tissue repair and regeneration. Am. J. Pathol., 185(10):2596-606, 2015.

- Degan, M.; Valle, L. D. & Alibardi, L. Gene expression in regenerating and scarring tails of lizard evidences three main key genes (wnt2b, egfl6, and arhgap28) activated during the regulated process of tail regeneration. *Protoplasma*, 258(1):3-17, 2021.
- Fischman, D. A. & Hay, E. D. Origin of osteoclasts from mononuclear leucocytes in regenerating newt limbs. *Anat. Rec.*, 143:329-37, 1962.
- He, B.; Song, H. & Wang, Y. Self-control of inflammation during tail regeneration of lizards. J. Dev. Biol., 9(4):48, 2021.
- Julier, Z.; Park, A. J.; Briquez, P. S. & Martino, M. M. Promoting tissue regeneration by modulating the immune system. *Acta Biomater*, 53:13-28, 2017.
- Könnecke, I.; Serra, A.; Khassawna, T. E.; Schlundt, C.; Schell, H.; Hauser, A.; Ellinghaus, A.; Volk, H.; Radbruch, A.; Duda, G. N.; et al. T and B cells participate in bone repair by infiltrating the fracture callus in a twowave fashion. Bone, 64:155-65, 2014.
- Kular, J.; Tickner, J.; Chim, S. M. & Xu, J. An overview of the regulation of bone remodelling at the cellular level. *Clin. Biochem.*, 45(12):863-73, 2012
- Landén, N.; Li, D. & Ståhle, M. Transition from inflammation to proliferation: a critical step during wound healing. *Cell. Mol. Life Sci.*, 73(20):3861-85, 2016.
- Londono, R.; Tighe, S.; Milnes, B.; DeMoya, C.; Quijano, L. M.; Hudnall, M. L.; Nguyen, J.; Tran, E.; Badylak, S. & Lozito, T. P. Single cell sequencing analysis of lizard phagocytic cell populations and their role in tail regeneration. J. Immunol. Regen. Med., 8:100029, 2020.
- Mescher, A.; Neff, A. & King, M. Inflammation and immunity in organ regeneration. Dev. Comp. Immunol., 66:98-110, 2017.
- Skaper, S.; Facci, L. & Giusti, P. Mast cells, glia and neuroinflammation: partners in crime? *Immunology*, 141(3):314-27, 2014.
- Tsai, S. The molecular interplay between progenitors and immune cells in tissue regeneration and homeostasis. J. Immunol. Regen. Med., 7:10024, 2020
- Vonk, A. C.; Zhao, X.; Pan, Z.; Hudnall, M. L.; Oakes, C. G.; Lopez, G. A.; Hasel-Kolossa, S.C.; Kuncz, A. W. C.; Sengelmann, S. B.; Gamble, D. J.; et al. Single-cell analysis of lizard blastema fibroblasts reveals phagocytedependent activation of Hedgehog-responsive chondrogenesis. Nat. Commun., 14(1):4489, 2023.
- Wu, P.; Alibardi, L. & Chuong, C. Regeneration of reptilian scales after wounding: neogenesis, regional difference, and molecular modules. *Regeneration (Oxf.)*, 1(1):15-26, 2014.
- Yang, C.; Sun, J.; Wang, X.; Yang, Y.; Chen, R. & Liu, B. Wnt1 and Wnt2b immunodetection of the regenerating tail and comparative ultrastructure of tail spinal cord in the *Scincella tsinlingensis*. *Int. J. Morphol.*, 40(5):1202-8, 2022b.
- Yang, C.; Wang, X.; Zhang, H.; Kou, Z.; Gao, Y.; He, Y.; & Liu, B. Microscopical observations on the regenerating tail of tsinling dwarf skink (Scincella tsinlingensis). Micron, 154:103215, 2022a.
- Yang, R. & Wu, L. Tissue location of macrophage during the gecko tail regeneration. Chin. J. Anat., 37(5):603-5, 2014.
- Zaiss, D. M. W.; Van Loosdregt, J.; Gorlani, A.; Bekker, C. P.; Gröne, A.; Sibilia, M.; van Bergen en Henegouwen, P. M.; Roovers, R. C.; Coffer, P. J. & Sijts, A. J. Amphiregulin enhances regulatory T cell-suppressive function via the epidermal growth factor receptor. *Immunity*, 38(2):275-84, 2013.
- Zhao, Y.; Li, L.; Kou, Z.; Gao, Y.; Shao, X. & Yang, C. Effect of a-asarone on cell proliferation during the stage of blastema formation in tail regeneration of *Scincella tsinlingensis*. *Chin. J. Wildl.*, *41*(1):165-70, 2020.

Corresponding author: Chun Yang, Prof. School of Life Sciences Shanxi Normal University Taiyuan Shanxi Province 030031 CHINA

E-mail: yangchun774@163.com